JOURNAL OF SOLID STATE CHEMISTRY **134,** 76–84 (1997)
ARTICLE NO. SC977538

Crystal Structure Refinement of $MgNb_2O_6$ Columbite from Neutron Powder Diffraction Data and Study of the Ternary System $MgO–Nb_2O_5–NbO$, with Evidence of Formation of New Reduced Pseudobrookite $Mg_{5-x}Nb_{4+x}O_{15-\delta}$ ($1.14 \leq x \leq 1.60$) Phases

S. Pagola and R. E. Carbonio[1]

INFIQC, Departamento de Fisicoquímica, Facultad de Ciencias Químicas, Universidad Nacional de Córdoba, Agencia Postal 4, CC 61, 5000 Córdoba, Argentina

J. A. Alonso

Instituto de Ciencia de Materiales de Madrid, Consejo Superior de Investigaciones Científicas, Cantoblanco, E-28049 Madrid, Spain

and

M. T. Fernández-Díaz

Institut Laue-Langevin, 156X, F-38042 Grenoble Cedex, France

Received November 18, 1996; in revised form July 8, 1997; accepted July 8, 1997

The crystal structure of the columbite-type phase $MgNb_2O_6$ has been refined from powder neutron diffraction data. The compound is orthorhombic, space group *Pbcn* (60), $Z = 4$, with unit cell parameters $a = 14.1875(1)$, $b = 5.7001(1)$, $c = 5.0331(1)$ Å. The structure contains chains of NbO_6 octahedra sharing edges along the *c* axis, which are arranged in double layers through common corners. The double layers, parallel to the *bc* plane, are connected via MgO_6 octahedra sharing corners. This compound contains Nb^{5+} with electronic configuration d^0. Attempts to obtain new materials with Nb in a mixed valence state were made in the ternary system $MgO–Nb_2O_5–NbO$. For molar ratios Mg : Nb = 1 : 2 new pseudobrookite-type phases have been identified. They have the general composition $Mg_{5-x}Nb_{4+x}O_{15-\delta}$, with *x* values ranging from 1.14 to 1.60. The compounds $Mg_4Nb_2O_{9-\delta}$ (corundum-type) and $Mg_3Nb_6O_{11}$ were identified when the Mg : Nb ratio was 4 : 2. All the reduced materials were also characterized by thermogravimetric analysis. © 1997 Academic Press

Key Words: **magnesium niobium oxides; columbite structure; neutron powder diffraction.**

INTRODUCTION

Recently there has been increased interest in Nb mixed oxides due to the appearance of some superconducting oxides, such as Li_xNbO_2 (1) and $Sr_{1-x}R_xNb_2O_6$ (R = rare earths) (2), containing Nb in a mixed-valence state, although superconductivity of the latter compound has not been reproduced by other groups. In these superconducting phases the formal oxidation state of niobium is lower than +5. Also, mixed oxides in which Nb presents an oxidation state between +4 and +5, such as Sr_xNbO_3 ($0.75 < x < 0.90$) and $BaNbO_3$, have also been investigated, although no superconducting behavior was reported (3, 4).

During the study of perovskite-related phases of composition $Ba_5Nb_4O_{15-x}$ (5) we found interesting electrical properties, making these oxides good candidates to search for new superconductors. Aiming to expand our research to the Mg–Nb–O system we first became involved in the study of some phases containing Nb^{5+} and subsequently explored the possibilities of preparation of new reduced compounds.

The phase diagram of the binary system $MgO–Nb_2O_5$ was first reported by Tilloca and Pérez y Jorba (6) and later confirmed by Abbattista *et al.* (7) and Brück *et al.* (8). Four compounds were reported: $Mg_4Nb_2O_9$, $Mg_{2/3}Nb_{11\,1/3}O_{29}$, $Mg_5Nb_4O_{15}$, and $MgNb_2O_6$.

[1] To whom correspondence should be addressed.

0022-4596/97 $25.00

$Mg_4Nb_2O_9$ shows a crystal structure derived from the ordering of Mg^{2+} and Nb^{5+} ions in the corundum-type (α-Al_2O_3) structure (9, 10). For $Mg_{2/3}Nb_{11\,1/3}O_{29}$, only phase equilibria and X-ray powder diffraction data are available in the literature (7, 8, 11). $Mg_5Nb_4O_{15}$ has a crystal structure related to that of the mineral pseudobrookite (Fe_2TiO_5) (12). For this composition we have recently shown (13) by Rietveld analysis of neutron powder diffraction data that there is a complete disordering of Mg^{2+} and Nb^{5+} over the two kinds of metal sites. The superstructure associated with the "tri-pseudobrookite" structure mentioned by Kasper (14) was not observed.

$MgNb_2O_6$ shows an orthorhombic columbite-type structure (12). A previous crystallographic study of this phase was done by Brandt (15). Eventhough single crystals of this compound have been prepared for optical studies (8, 16, 17), there is a lack of accurate structural information on this compound. The first part of this paper is concerned with establishing the fine-structural features of $MgNb_2O_6$, from a high-resolution powder neutron diffraction study.

Very little is known about the ternary phase diagram $MgO–Nb_2O_5–NbO$. Abbattista and Rolando (18) reported that they could not obtain reduced phases from $MgNb_2O_6$ (white electrical insulator) by heating this compound at high temperatures in reducing atmospheres such as H_2 and CO. They achieved preparation of the reduced compound $Mg_3Nb_6O_{11}$ by heating at 1100°C stoichiometric mixtures of MgO, Nb, and NbO_2 in sealed quartz ampoules. Marinder (19) also reported the synthesis of $Mg_3Nb_6O_{11}$, starting from $MgO–NbO_2$ mixtures with different Mg : Nb ratios. The compound contains Nb_6O_{12} isolated niobium clusters and has semiconducting properties (20, 21).

In the present work, attempts to obtain new compounds containing Nb in a reduced or mixed-valence oxidation state have been made in the ternary system $MgO–Nb_2O_5–NbO$. The second part of this paper reports the results of the synthesis processes of materials with Mg : Nb ratios 1 : 2 and 4 : 2. We also present a partial phase diagram for the ternary system $MgO–Nb_2O_5–NbO$.

EXPERIMENTAL

$MgNb_2O_6$ has been synthesized as a white polycrystalline powder by heating in air a stoichiometric mixture of analytical grade MgO and Nb_2O_5 at 1150°C for 24 h. The sample was reground and the process repeated to improve homogeneity and crystallinity.

Two series of reduced compounds with Mg : Nb ratios of 1 : 2 and 4 : 2 were prepared. The starting materials, MgO, Nb_2O_5, and Nb metal powder, were pressed into pellets and heated in evacuated quartz ampoules at 1150°C for 24 h.

For a Mg : Nb ratio of 1 : 2, the nominal solid-state reaction can be written as

$$a\text{Nb} + b\text{Nb}_2\text{O}_5 + \text{MgO} \rightarrow \text{MgNb}_2\text{O}_{6-x}, \quad [1]$$

where

$$a + 2b = 2. \quad [2]$$

When the Mg : Nb ratio is 4 : 2, the nominal reaction is:

$$c\text{Nb} + d\text{Nb}_2\text{O}_5 + 4\text{MgO} \rightarrow \text{Mg}_4\text{Nb}_2\text{O}_{9-x}, \quad [3]$$

where

$$c + 2d = 2. \quad [4]$$

In Eqs. [1] and [3] the formulas $MgNb_2O_{6-x}$ and $Mg_4Nb_2O_{9-x}$ just indicate the overall elemental compositions of the final materials.

Thermogravimetric analysis (TGA) of the dark reduced samples was performed in Mettler TA3000 equipment. The average oxidation states (AOSs) of niobium on the final materials were obtained by heating the samples in air up to 900°C, according to the following reactions:

$$\text{MgNb}_2\text{O}_{6-x} + (x/2)\text{O}_2 \rightarrow \text{MgNb}_2\text{O}_6, \quad [5]$$

$$\text{Mg}_4\text{Nb}_2\text{O}_{9-x} + (x/2)\text{O}_2 \rightarrow \text{Mg}_4\text{Nb}_2\text{O}_9. \quad [6]$$

Formation of the fully oxidized columbite and corundum phases, white in color, after the oxidation process was verified by X-ray diffraction.

X-ray powder diffraction (XRD) patterns were recorded in a PW-170 Phillips diffractometer using $K\alpha$ radiation, scanning from 10° to 75° 2θ, with steps of 0.02°.

Neutron powder diffraction (NPD) data of $MgNb_2O_6$ were collected at room temperature in the high-resolution D2B diffractometer at ILL, Grenoble, by step-scanning between 0° and 162° 2θ with increments of 0.05°. A wavelength of 1.594 Å was selected from a Ge monochromator. About 10 g of sample was contained in a cylindrical vanadium can. The counting time was approximately 3 h.

All the diffraction patterns were analyzed by the Rietveld method, using a strongly modified version (22) of Wiles and Young's refinement program (23) (neutron data) and the DWS-9411-PC (24) (X-ray data) program. For the NPD diagram the following parameters were refined: background coefficients, zero point, half-width, pseudo-Voigt and asymmetry parameters for the peak shape, scale factor, atomic positions, thermal anisotropic factors, and unit cell parameters. No regions were excluded in the refinement. In the XRD refinements a Pearson VII function was used to generate the peak shape. A multipattern refinement was performed when two or more phases were identified in the XRD diagrams. Zero point and background were refined for the whole pattern. Half-width, scale, asymmetry, Pearson VII mixing parameters for the peak shape, overall isotropic temperature factors, atomic positions, and cell parameters for each phase were refined. From the refined scale factors the molar fractions of the different phases in the mixture were determined using as a restriction the overall molar relation Mg : Nb 1 : 2.

RESULTS AND DISCUSSION

1. Structural Refinement of $MgNb_2O_6$

Both X-ray and neutron diffraction diagrams of $MgNb_2O_6$ could be indexed on the basis of a simple columbite cell, with orthorhombic unit cell parameters $a = 14.1875(1)$, $b = 5.7001(1)$, $c = 5.0331(1)$ Å. No additional peaks, which could indicate the presence of superstructures or departure of the mentioned symmetry, were observed in the patterns.

The atomic positions of the mineral columbite, (Fe, Mn) Nb_2O_6 (12), were used as starting parameters in the Rietveld refinement of the NPD data. The space group *Pbcn* was considered, $Z = 4$. The final atomic coordinates, anisotropic thermal factors, and discrepancy factors after the refinement are listed in Table 1. The fact that the anisotropic temperature factors β_{11} in Table 1 are a magnitude smaller than β_{22} and β_{33} is coherent with the considerably larger value of the *a* unit cell parameter with respect to *b* and *c*, since the magnitudes of the three major axes of the vibration ellipsoids are proportional to the products of $a^2 \cdot \beta_{11}$, $b^2 \cdot \beta_{22}$, and $c^2 \cdot \beta_{33}$, respectively. The excellent agreement between the observed and calculated profiles of the pattern is shown in Fig. 1. Final bonding distances and angles are given in Table 2.

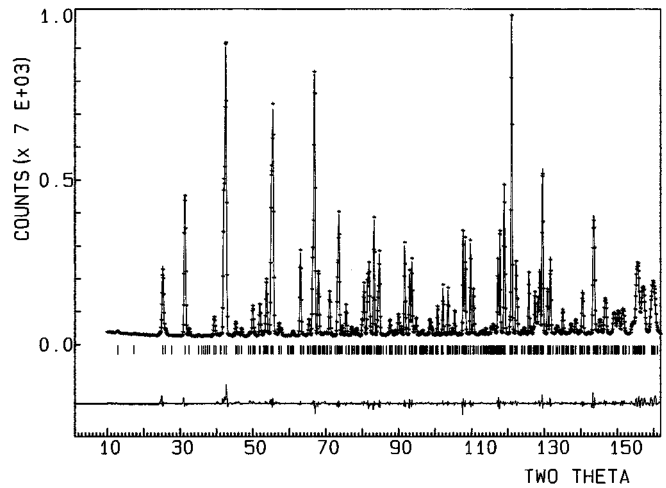

FIG. 1. Observed (crosses), calculated (solid line), and difference (at bottom) neutron diffraction profiles for $MgNb_2O_6$ at 295 K. The series of tick marks indicates the allowed Bragg reflections. For the sake of clarity, only half of the experimental points are represented.

TABLE 1
Atomic Parameters, Anisotropic Thermal Factors (×10⁴), and Discrepancy Factors after the Refinement of NPD Data for $MgNb_2O_6$ at 295 K (Space Group *Pbcn*, $Z=4$)[a]

Atom	Site	x	y	z	B_{eq} (Å^2)
Mg	4*c*	0	0.1688(5)	0.25	0.40(3)
Nb	8*d*	0.15993(8)	0.3181(2)	0.7538(3)	0.24(1)
O1	8*d*	0.0955(1)	0.3944(3)	0.4321(3)	0.37(3)
O2	8*d*	0.0796(1)	0.1163(4)	0.9077(4)	0.25(2)
O3	8*d*	0.2560(1)	0.1222(3)	0.5833(4)	0.33(2)

Atom	β_{11}	β_{22}	β_{33}	β_{12}	β_{13}	β_{23}
Mg	3.8(4)	49(4)	33(4)	0	− 1(2)	0
Nb	2.8(2)	14(2)	28(2)	1(1)	5(1)	11(4)
O1	6.7(4)	25(3)	33(3)	− 1(2)	− 4(2)	11(4)
O2	4.8(3)	63(3)	32(3)	− 6(2)	1(2)	1(5)
O3	5.1(3)	13(3)	29(3)	6(2)	6(2)	− 2(5)

[a] Discrepancy factors: $R_{wp} = 4.83$, $R_p = 3.61$, $R_{exp} = 2.01$, $R_I = 2.49\%$; $\chi^2 = 5.8$.

TABLE 2
Selected Interatomic Distances (Å) and Angles (Degrees) for $MgNb_2O_6$

Mg–O1	2.081(3) × 2	Nb–O1	1.910(2)
–O2	2.081(2) × 2	–O1	2.080(2)
–O2	2.132(3) × 2	–O2	1.795(2)
⟨Mg–O⟩	2.098(1)	–O3	1.960(2)
		–O3	2.273(2)
		–O3	2.071(3)
		⟨Nb–O⟩	2.015(1)
O1–Mg–O1	103.6(1)	Mg–O1–Nb	123.0(2)
–Mg–O2	95.8(1)	–O1– Nb	125.7(2)
–Mg–O2	87.8(1)	Nb–O1–Nb	109.6(1)
–Mg–O2	94.4(1)	Mg–O2–Mg	97.5(2)
–Mg–O2	168.5(12)	–O2–Nb	127.6(2)
O2–Mg–O2	84.9(1)	–O2–Nb	131.6(3)
–Mg–O2	163.5(7)	Nb–O3–Nb	129.4(2)
–Mg–O2	82.5(1)	–O3–Nb	131.1(3)
–Mg–O2	80.7(1)	–O3–Nb	97.2(1)
O1–Nb–O1	88.6(1)	O2–Nb–O3	105.4(2)
–Nb–O2	102.0(2)	–Nb–O3	170.1(14)
–Nb–O3	95.3(1)	–Nb–O3	97.2(2)
–Nb–O3	76.0(1)	O3–Nb–O3	84.5(1)
–Nb–O3	156.5(6)	–Nb–O3	92.5(2)
–Nb–O2	92.3(2)	–Nb–O3	82.8(1)
–Nb–O3	160.6(7)		
–Nb–O3	78.0(1)		
–Nb–O3	77.2(1)		

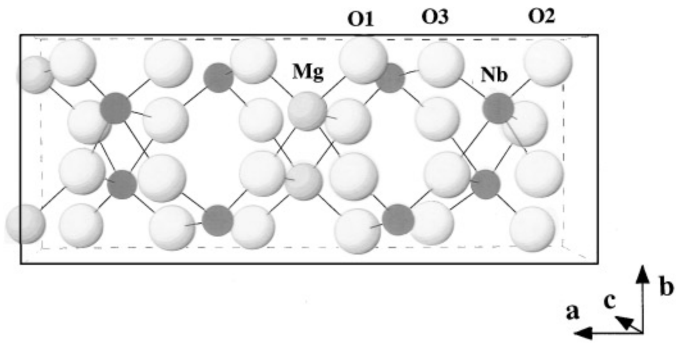

FIG. 2. Unit cell content of $MgNb_2O_6$.

Figure 2 shows the content of the unit cell, and a view of the structure projected along *c* is shown in Fig. 3. Both Mg and Nb atoms are hexacoordinated to oxygens. MgO_6 and NbO_6 units can be considered fairly distorted octahedra, with Mg–O distances between 2.08 and 2.13 Å and Nb–O bond lengths ranging from 1.80 to 2.27 Å. Average ⟨Mg–O⟩ and ⟨Nb–O⟩ bonding distances agree with the expected values calculated as ionic radius sums (25), 2.12 and 2.04 Å, respectively.

The structure can be described as follows: NbO_6 octahedra share edges via O1 and O3, forming zig-zag chains along the *c* axis; the octahedra of adjacent chains share corners via O3 to form double layers parallel to the *bc* plane, as shown in Fig. 3. The double layers are linked together along the [100] direction through MgO_6 units, via O1 and O2 oxygens in common corners, giving rise to a three-dimensional array. Observe that MgO_6 octahedra also share edges to form zig-zag chains along the *c* axis.

The oxidation state of both metal cations, Mg^{2+} and Nb^{5+}, is in the origin of the insulating behavior of $MgNb_2O_6$. The fact that Nb^{5+} cations can be rather easily reduced to Nb^{4+}, with an ionic radius (0.68 Å) very close to

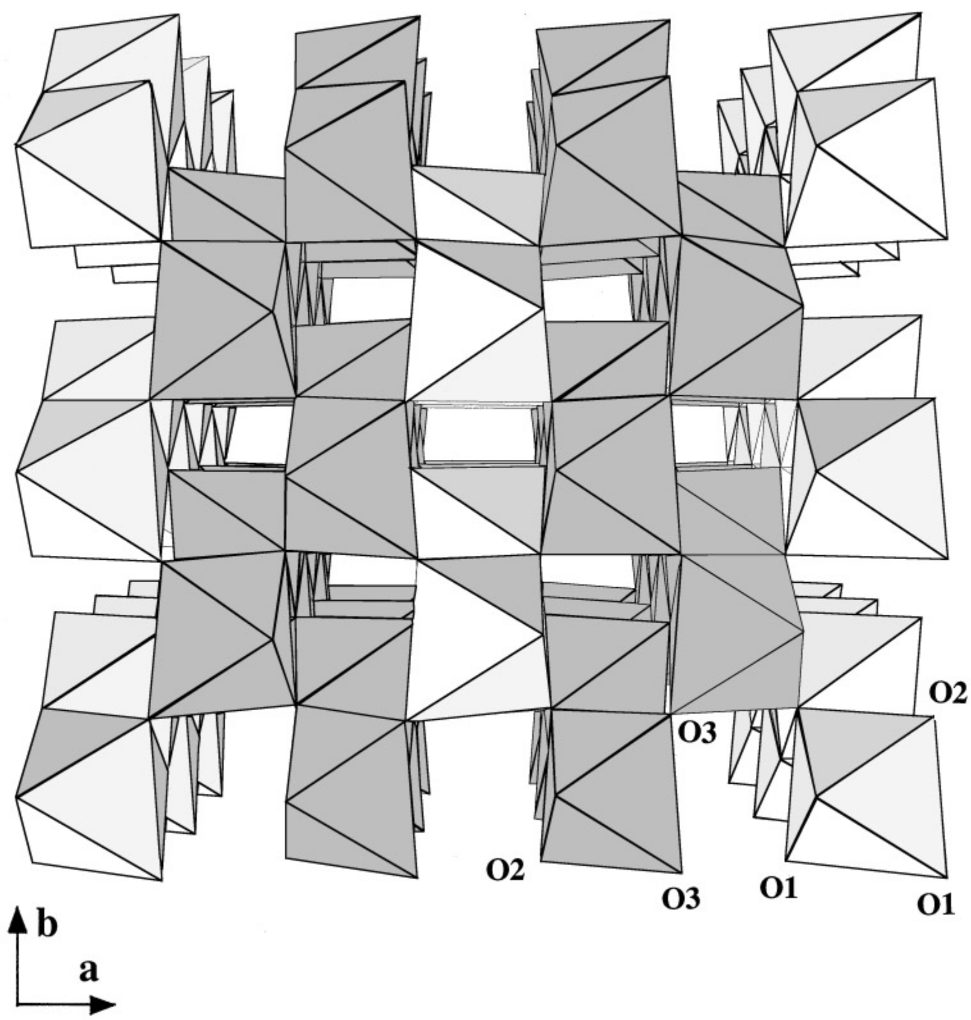

FIG. 3. View of the $MgNb_2O_6$ structure projected along the [001] axis. Shaded and unshaded octahedra represent NbO_6 and MgO_6 octahedra, respectively.

that of Nb^{5+} (0.64 Å) (25), suggests the possibility of formation of reduced compounds in phases of stoichiometry $MgNb_2O_{6-\delta}$, with the Nb^{4+}/Nb^{5+} ratio increasing with δ. The mixed-valence Nb^{4+}–Nb^{5+} in the hypothetical intermediate phases suggests interesting electrical and magnetic properties for these compounds, based on the columbite structure.

2. *Reduced Phases in the MgO–Nb_2O_5–NbO System*

The different phases obtained from MgO–Nb_2O_5–Nb mixtures were characterized by X-ray diffraction and TGA measurements. The *a*/*b* or *c*/*d* ratios of the stoichiometric coefficients for Nb and Nb_2O_5 in Eqs. [1] and [3], as well as the AOS values and the phases identified by XRD are

TABLE 3
***a*/*b*, Experimental AOS Identified Phases with Their Cell Parameters, R_I, and Molar Fraction (*f*) Values for Each Phase, as Well as the Different *R* Values for the Multiphase Pattern Refinement**

a/*b*	AOS	$MgNb_2O_{6-\delta}$	NbO_2	Pseudobrookite	$Mg_3Nb_6O_{11}$	NbO	MgO	*R* factors
0.092	~ +5	$R_I = 6.42$ $a = 14.1866(3)$ $b = 5.7005(1)$ $c = 5.0331(1)$						$R_{wp} = 24.89$ $R_p = 17.29$ $R_{exp} = 18.73$ $S = 1.33$
0.193	~ +5	$R_I = 5.13$ $a = 14.1875(2)$ $b = 5.70037(9)$ $c = 5.03355(8)$						$R_{wp} = 24.38$ $R_p = 16.48$ $R_{exp} = 18.10$ $S = 1.35$
0.304	+4.96	$R_I = 5.41$ $a = 14.1849(2)$ $b = 5.69824(9)$ $c = 5.03201(8)$ $f = 0.93$	$R_I = 13.70$ $a = 4.7997(4)$ $c = 3.0274(3)$ $f = 0.07$					$R_{wp} = 23.63$ $R_p = 15.99$ $R_{exp} = 17.59$ $S = 1.34$
0.427	+4.51	$R_I = 10.25$ $a = 14.1863(6)$ $b = 5.6987(2)$ $c = 5.0330(2)$ $f = 0.22$	$R_I = 4.83$ $a = 4.7932(2)$ $c = 3.0328(1)$ $f = 0.54$	$R_I = 9.87$ $a = 3.8063(2)$ $b = 10.0530(6)$ $c = 10.2579(6)$ $f = 0.24$				$R_{wp} = 22.97$ $R_p = 16.49$ $R_{exp} = 18.21$ $S = 1.26$
0.564	+4.18		$R_I = 5.00$ $a = 4.7988(1)$ $c = 3.02830(8)$ $f = 0.72$	$R_I = 10.97$ $a = 3.8065(1)$ $b = 10.0540(4)$ $c = 10.2570(4)$ $f = 0.28$				$R_{wp} = 22.93$ $R_p = 16.32$ $R_{exp} = 18.02$ $S = 1.27$
0.886[a]	+3.57		$R_I = 2.89$ $a = 4.8006(1)$ $c = 3.02868(9)$ $f = 0.65$	$R_I = 9.14$ $a = 3.8072(1)$ $b = 10.0585(4)$ $c = 10.2597(4)$ $f = 0.31$	$R_I = 7.60$ $a = 6.0413(1)$ $c = 7.4657(3)$ $f = 0.04$			$R_{wp} = 20.85$ $R_p = 14.88$ $R_{exp} = 17.64$ $S = 1.18$
1.333[a]	+3.46		$R_I = 4.80$ $a = 4.7985(2)$ $c = 3.0296(1)$ $f = 0.66$	$R_I = 12.97$ $a = 3.8055(2)$ $b = 10.0524(6)$ $c = 10.2557(6)$ $f = 0.29$	$R_I = 9.35$ $a = 6.0391(1)$ $c = 7.4635(3)$ $f = 0.05$			$R_{wp} = 23.10$ $R_p = 16.84$ $R_{exp} = 18.21$ $S = 1.27$
1.589[a]	+3.05		$R_I = 5.19$ $a = 4.8011(2)$ $c = 3.0279(2)$ $f = 0.41$	$R_I = 9.32$ $a = 3.8067(1)$ $b = 10.0544(4)$ $c = 10.2552(4)$ $f = 0.40$	$R_I = 7.20$ $a = 6.04023(8)$ $c = 7.4635(1)$ $f = 0.12$	$R_I = 9.03$ $a = 4.2094(1)$ $f = 0.07$		$R_{wp} = 22.83$ $R_p = 16.13$ $R_{exp} = 17.75$ $S = 1.29$
1.906[a]	+2.48				$R_I = 5.84$ $a = 6.04051(9)$ $c = 7.4657(1)$ $f = 0.385$	$R_I = 10.96$ $a = 4.2100(1)$ $f = 0.33$	$R_I = 14.15$ $a = 4.2155(5)$ $f = 0.285$	$R_{wp} = 22.42$ $R_p = 15.27$ $R_{exp} = 18.06$ $S = 1.24$

[a] Nb metal powder pressed into a pellet, present in the ampoule as oxygen getter.

TABLE 4
***c/d*, Experimental AOS and Identified Phases in Samples with the Ratio Mg:Nb=4:2**

c/d	AOS	Identified phases	Cell parameters for $Mg_4Nb_2O_{9-\delta}$
0	+ 5	$Mg_4Nb_2O_9$	$a = 5.157(2)$, $c = 13.987(9)$
[a]	+ 4.52	$Mg_4Nb_2O_{8.52}$	$a = 5.147(2)$, $c = 13.980(6)$
0.50	+ 4.00	$Mg_4Nb_2O_{9-\delta}$, $Mg_3Nb_6O_{11}$, MgO	$a = 5.156(1)$, $c = 13.97(1)$

[a] Obtained from NbO_2 and MgO.

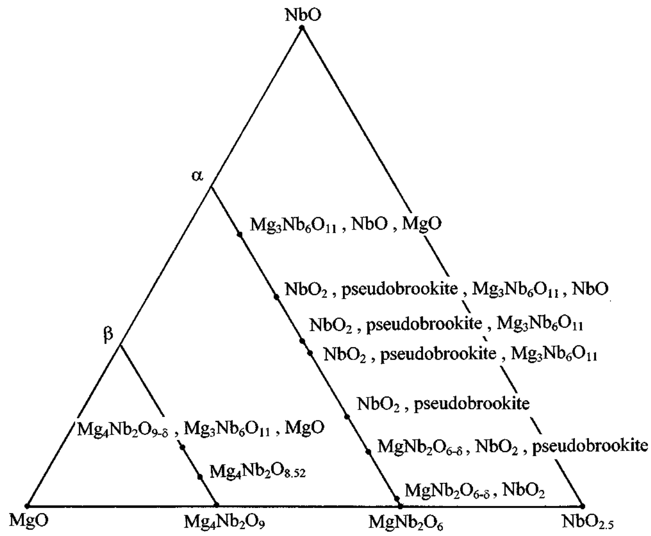

FIG. 4. Partial ternary phase diagram for the system $MgO–Nb_2O_5–NbO$ (samples synthetized at $T = 1150°C$).

presented in Tables 3 and 4. A multipattern refinement of the XRD profiles of samples with Mg : Nb ratios of 1 : 2 was performed. The molar fractions (f) of the different compounds were determined from the refined scale factors and are listed in Table 3 together with the R factors for the multiphase refinement of the whole pattern and R_I and refined cell parameters for each phase. The identified phases are also shown in a ternary phase diagram (Fig. 4) along α and β lines for Mg : Nb ratios of 1 : 2 and 4 : 2, respectively. A plot of the f values for each phase versus AOS is shown in Fig. 5. Except for the pseudobrookite phase, a maximum value of f is observed when the AOS is in the vicinity of the oxidation state of Nb for that phase (oxidation state of Nb in each phase is shown by an arrowhead on top of the figure).

2.1. Starting mixtures with Mg : Nb = 1 : 2. A plot showing a linear relationship between the a/b ratio and the AOS observed in these phases is shown in Fig. 6. In all cases the experimental oxidation state was greater than that expected for the stoichiometry of the starting mixtures. This may be explained considering that the ampoule contains a residual amount of oxygen that contributes to oxidize the samples during the thermal treatments. According to this plot it is possible to tune the AOS in the final products by controlling the a/b ratio of the starting mixtures of reactants.

For a/b values up to 0.193 (see Table 3) the columbite $MgNb_2O_{6-\delta}$ was identified as a single phase by XRD. This suggests that it is possible to introduce a small concentration of oxygen vacancies (δ) into this phase without destroying the crystal structure. Despite the fact that the observed AOS values were very close to $+5$ (i.e., there was no measurable mass gain in the TGA curves in air), a certain degree of reduction for this sample could be inferred from the gray color of the materials. A similar effect has been observed in single crystals of $MgNb_2O_6$, blue in color due to the generation of oxygen vacancies during the synthesis under reducing conditions (17). Also, a gray color was observed after treatment of polycrystalline $MgNb_2O_6$ at 1150°C in a 10% H_2 + 90% Ar atmosphere.

For increasing a/b ratios, mixtures of $MgNb_2O_{6-\delta}$, a pseudobrookite-type phase, and a rutile phase were obtained. The presence of a rutile-type compound was previously reported (19), and could be identified in the present work as the tetragonal form of NbO_2 (26). For AOS values equal to or lower than $+3.57$, the formation of $Mg_3Nb_6O_{11}$ is observed; in the most reduced samples, NbO could also be identified.

The nature of the identified pseudobrookite phases needs to be discussed. Recently, we prepared and refined the crystal structure of stoichiometric $Mg_5Nb_4O_{15}$, adopting this structural type (13). We proposed (13) that $Mg_5Nb_4O_{15}$ is a particular composition of the more general formula $Mg^{2+}_{5-x}Nb^{m+}_{4+x}O_{15-\delta}$, adopting the pseudobrookite structure, where the niobium oxidation state varies from $m = +5$ for $x = 0$ to $m = +4$ for $x = 2$ (if $\delta = 0$).

By including the crystallographic model of $Mg_5Nb_4O_{15}$ in the Rietveld analysis of the XRD patterns of the reaction products we obtained the molar fractions of the pseudobrookite phase listed in Table 3. From the relative molar fractions of the present phases we could determine the actual composition of the pseudobrookite phase, taking into account that the Mg : Nb ratio has to be 1 : 2 in the final mixture. Oxygen balance was not considered since at least two phases, $Mg^{2+}_{5-x}Nb^{m+}_{4+x}O_{15-\delta}$ and $MgNb_2O_{6-\delta}$, are oxygen deficient with an unknown amount of oxygen deficiencies. The compositions thus derived are listed in Table 5. Cell parameters and cell volumes for these phases are shown in Fig. 7 as a function of x. Changes in these values are within the experimental errors, so we can conclude that at least in this range of compositions there are no appreciable changes in cell parameters. This seems reasonable not only

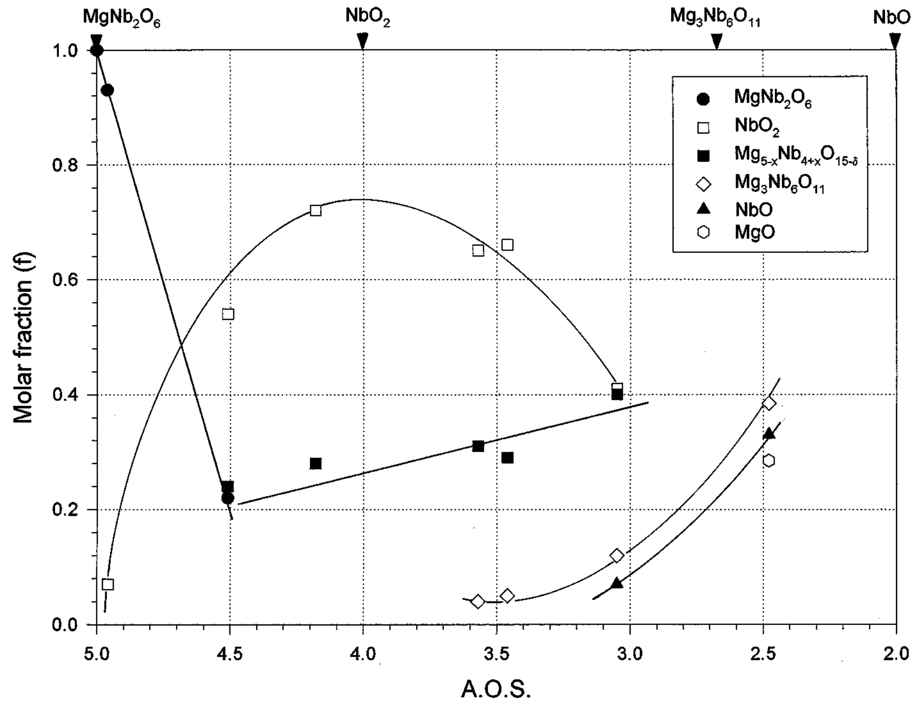

FIG. 5. Molar fractions (f) of the different phases obtained with molar ratios Mg: Nb 1: 2 versus AOS.

because the composition range is small but also because the ionic radii of Mg^{2+} (0.72 Å) and Nb^{4+} (0.68 Å) are very similar. We thus show evidence, of the existence of pseudo-brookite-type phases with a stoichiometry different from that previously described, $Mg_5Nb_4O_{15}$. The ability of this structure to incorporate at random Mg and Nb atoms in both metal positions makes it possible to tune the oxidation state of Nb by appropriate control of the Mg and Nb

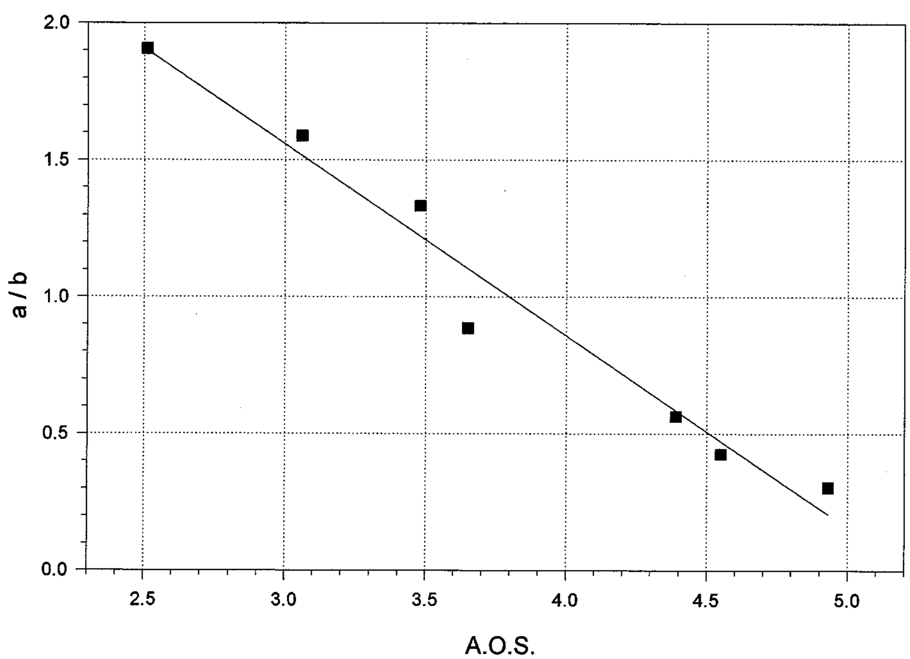

FIG. 6. a/b values in Eq. [1] versus observed AOS for final materials with Mg: Nb ratios of 1: 2.

TABLE 5
Composition of the Identified Pseudobrookite Compounds

a/b	AOS	Composition of pseudobrookite
0.427	+ 4.51	$Mg_{3.68}Nb_{5.32}O_{15-\delta}$
0.564	+ 4.18	$Mg_{3.86}Nb_{5.14}O_{15-\delta}$
0.886	+ 3.57	$Mg_{3.70}Nb_{5.30}O_{15-\delta}$
1.333	+ 3.46	$Mg_{3.76}Nb_{5.24}O_{15-\delta}$
1.589	+ 3.05	$Mg_{3.40}Nb_{5.60}O_{15-\delta}$

contents and δ in the structure. In the present work, we could identify $Mg_{5-x}Nb_{4+x}O_{15-\delta}$ compositions with $1.14 \leq x \leq 1.60$ and unknown δ values.

2.2. Starting mixtures with Mg : Nb = 4 : 2. When the ratio Mg : Nb is 4 : 2 the phase $Mg_4Nb_2O_{8.52}$ is obtained (see Table 4), for which the experimental AOS is +4.52. This suggests that the corundum-type structure can accept a large number of oxygen vacancies and, therefore, a high content of Nb^{4+} in the structure. For an AOS of +4.00 a mixture of phases was obtained. Cell parameters for $Mg_4Nb_2O_{9-\delta}$ hardly change with AOS (Table 4). Despite the fact that Nb^{4+} can be easily formed in this structure, given the absence of connectivity between NbO_6 octahedra in the corundum structure (10), poor electrical conductivities are to be expected in these reduced $Mg_4Nb_2O_{9-\delta}$ phases.

CONCLUSIONS

The crystal structure of $MgNb_2O_6$ columbite has been refined from high-resolution neutron diffraction data. MgO_6 and NbO_6 octahedra share edges to form zig-zag chains running along the *c* axis. NbO_6 octahedra of adjacent chains share corners to give double layers parallel to the *bc* plane. Such double layers are connected through MgO_6 octahedra via common corners.

The study of a set of reduced materials with Mg:Nb ratios of 1 : 2 enabled us to identify new pseudobrookite-type phases of general composition $Mg_{5-x}Nb_{4+x}O_{15-\delta}$ with *x* values ranging from 1.14 to 1.60.

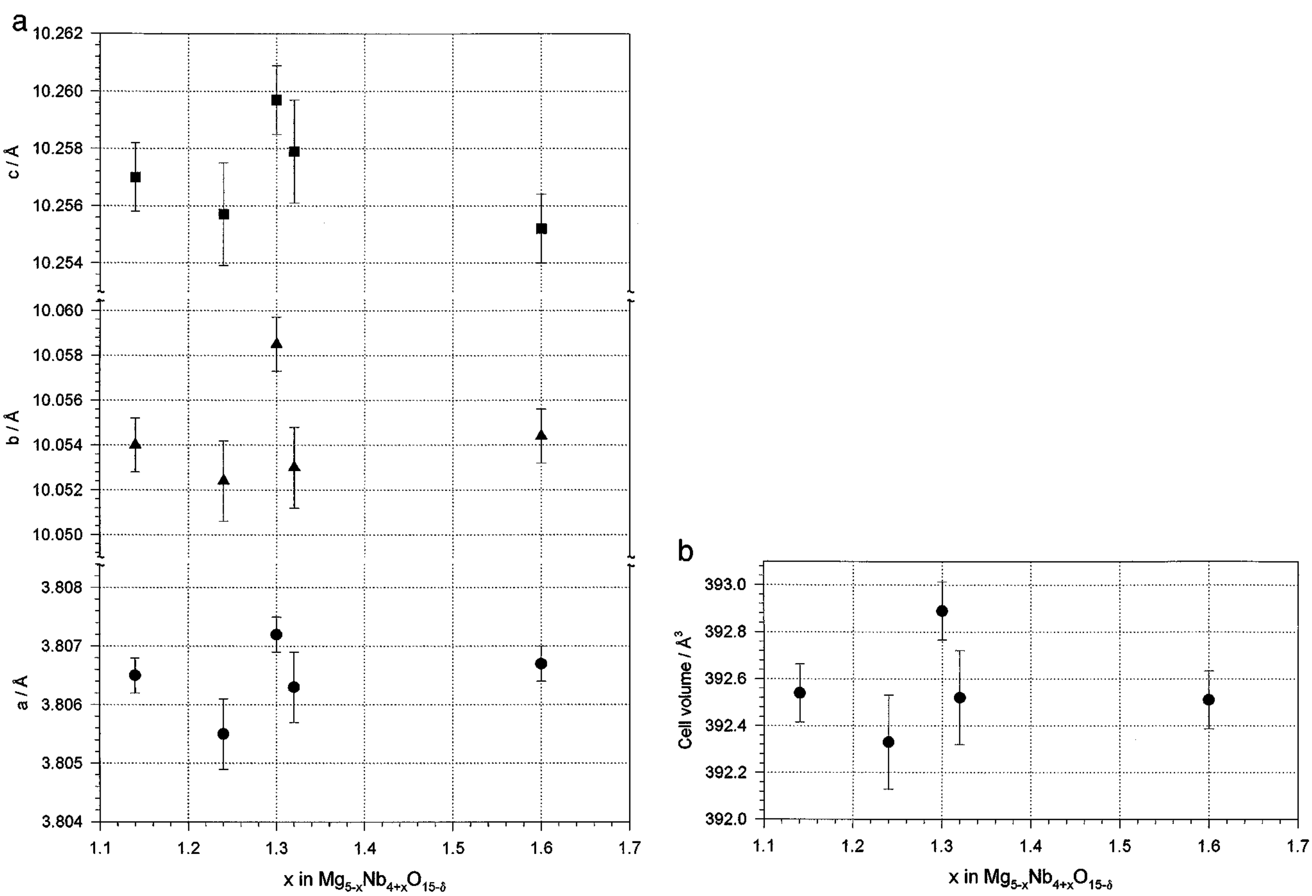

FIG. 7. (a) Refined cell parameters versus *x* for $Mg_{5-x}Nb_{4+x}O_{15-\delta}$. (b) Cell volume versus *x* for $Mg_{5-x}Nb_{4+x}O_{15-\delta}$.

ACKNOWLEDGMENTS

R.E.C. thanks the Consejo de Investigaciones Científicas y Tecnológicas de la Provincia de Córdoba (CONICOR), Secretaría de Ciencia y Tecnología of the Universidad Nacional de Córdoba, and Fundación Antorchas for Research Grants. This research was partly supported by a Joint Research Project CSIC/CONICET. S.P. thanks CONICET for a fellowship. J.A.A. acknowledges the financial support of the Spanish DGICYT to Project PB94-0046.

REFERENCES

1. M. J. Geselbracht, T. J. Richardson, and A. M. Stacy, *Nature* **345,** 324 (1990).
2. J. Akimitsu, J. Amano, H. Sawa, O. Nagase, K. Gioda, and M. Kogai, *Jpn. J. Appl. Phys.* **30,** L1155 (1991).
3. M. T. Casais, J. A. Alonso, I. Rasines, and M. A. Hidalgo, *Mater. Res. Bull.* **30,** 201 (1995).
4. K. Isawa, J. Sugiyama, K. Matsuura, A. Nozaki, and H. Yamauchi, *Phys. Rev. B* **47,** 2849 (1993).
5. S. Pagola, N. E. Massa, G. Polla, G. Leyva, and R. E. Carbonio, *Physica C* **235–240,** 755 (1994).
6. G. Tilloca and M. Pérez y Jorba, *C. R. Acad. Sci. Paris* **226,** 906 (1968).
7. F. Abbattista, P. Rolando, and G. Borroni Grassi, *Ann. Chim.* (*Rome*) **60,** 425 (1970).
8. E. Brück, R. K. Route, R. J. Raymakers, and R. S. Feigelson, *J. Cryst. Growth* **128,** 842 (1993).
9. W. Wong-Ng, H. F. McMurdie, B. Paretzkin, C. R. Hubbard, A. L. Dragoo, and J. M. Stewart, *Powder Diffraction* **2,** No. 2 (1987).
10. E. F. Bertaut, L. Corliss, F. Forrat, R. Aleonard, and R. Pauthenet, *J. Phys. Chem. Solids* **21,** 234 (1961).
11. R. Norin, C. Arbin, and B. Nolander, *Acta Chem. Scand.* **26,** 3389 (1972).
12. R. W. G. Wyckoff, "Crystal Structures," 2nd ed., Interscience, New York, 1964.
13. S. Pagola, J. A. Alonso, R. E. Carbonio, and M.T. Fernández-Díaz, *J. Solid State Chem.*, submitted.
14. H. Kasper, *Z. Anorg. Allg. Chem.* **354,** 208 (1967).
15. K. Brandt, *Ark. Kemi Min. Geol.* **17A,** No. 15 (1943).
16. C. Zaldo, M. J. Martín, C. Coya, K. Polgár, A. Péter, and J. Paitz, *J. Phys: Condensed Matter* **7,** 2249 (1995).
17. K. Polgár, A. Péter, J. Pitz, and C. Zaldo, *J. Cryst. Growth* **151,** 365 (1995).
18. F. Abbattista and P. Rolando, *Ann. Chim.* **61,** 196 (1971).
19. B. O. Marinder, *Chem. Scr.* **11,** 97 (1977).
20. R. Burnus, J. Köeler, and A. Simon, *Z. Naturforsch. B* **42,** 536 (1987).
21. J. Köeler, G. Svensson, and A. Simon, *Angew. Chem. Int. Ed. Engl.* **31,** 1437 (1992).
22. J. Rodríguez-Carvajal, *Physica B* **192,** 55 (1993).
23. B. Wiles and R. A. Young, *J. Appl. Crystallogr.* **14,** 149 (1981).
24. R. A. Young, A. Sakthivel, T. S. Moss, and C. O. Paiva-Santos, *J. Appl. Crystallogr.* **28,** 366 (1995).
25. R. D. Shannon, *Acta Crystallogr. Sect. A* **32,** 751 (1976).
26. F. S. Galasso, "Structure and Properties of Inorganic Solids." Pergamon, Oxford, 1970.